

Where Does Vision Meet Language?

Understanding and Refining Visual Fusion in MLLMs via Contrastive Attention

Shezheng Song, Shasha Li, Jie Yu

¹ National University of Defense Technology

Abstract

Recent advances in Multimodal Large Language Models (MLLMs) have achieved impressive results in vision-language tasks. However, the internal mechanism of how visual information is integrated across layers remains poorly understood. In this work, we investigate the hierarchical process of visual integration in MLLMs through a series of layer-wise masking experiments. Our findings reveal that vision-language fusion primarily occurs at several shallow layers. We also discover a review-like behavior at a deep layer, where the model re-attends to the image before producing the final output. We further analyze attention distributions and uncover a systematic bias: irrelevant image regions often receive consistently high attention across layers, resulting in noisy and suboptimal final predictions. To address this issue, we propose a training-free method that leverages contrastive attention, defined as the difference in attention maps between a pre-integrated layer and a post-integrated layer. This captures the evolving focus of the model as it integrates visual information. We apply the contrastive attention at the review layer to selectively mask irrelevant image regions, guiding the model to attend more effectively to task-relevant content without requiring additional training. Extensive experiments on multiple multimodal benchmarks demonstrate that our method significantly boosts performance, achieving new state-of-the-art results on the LLaVA series. The code will be released.

1 Introduction

In recent years, Multimodal Large Language Models (MLLMs) (Liu et al. 2023; Bai et al. 2023) have shown strong performance on tasks such as visual question answering (Goyal et al. 2017; Marino et al. 2019). However, how information flows between layers in MLLMs, especially how visual signals are gradually integrated and utilized across layers, has not been fully explored. This gap in understanding limits the development of effective training strategies and model architectures.

To address this gap, we focus on the internal process of visual-textual information fusion: At which layers is visual information integrated, and how does integration in each layer affect task performance? To explore this, we design a series of layer-wise masking experiments to systematically

evaluate the role of each layer in cross-modal fusion. Specifically, we apply masking to visual feature at different layers and observe the resulting changes in model performance and inference speed. A significant performance drop after masking indicates that the corresponding layer plays a critical role in visual integration, whereas a minimal impact suggests a weaker dependence on visual information. This approach provides a functional perspective on the hierarchical dynamics of vision-language fusion in MLLMs. Our experiments show that visual-text fusion mainly happens at several shallow layers. Masking visual inputs at these layers causes performance to drop nearly to zero, highlighting their role as **fusion layers**. This effect is consistent across different datasets and MLLMs, showing stable layer-wise patterns. As depth increases, masking has less impact, suggesting that visual information has already been integrated. Notably, a sharp drop reappears at a late layer (e.g., layer 29), indicating the model briefly revisits the image before producing the final output. We call this a **review mechanism**, and the corresponding layer the review layer.

In addition to analyzing the functional roles of each layer through masking, we further investigate how visual attention is distributed across layers. This analysis reveals a fundamental issue in current MLLMs: **Systematic bias in visual attention allocation**. As illustrated in Figure 1, the final layer often fails to accurately attend to regions in the image that are truly relevant to the question. Prior work such as Zhang et al. (2025) has noted this limitation and attempted to address it by directly using attention maps from a fixed intermediate layer (e.g., layer 14 in LLaVA (Liu et al. 2023), layer 15 in InstructBLIP (Dai et al. 2023)). However, relying on a single fixed layer is both rigid and suboptimal, as it overlooks the dynamic nature of visual reasoning across tasks and model architectures. Furthermore, we observe that some irrelevant image regions consistently receive high attention across layers, a phenomenon we refer to as **high-attention noise**. These regions tend to be activated in early layers and remain prominent in later ones. For example, as shown in Figure 1, the yellow dashed region maintains high attention values from shallow to deep layers, despite its irrelevance to the question. This layer-to-layer consistency suggests that early attention biases may propagate through the network and contribute to the suboptimal final attention patterns.

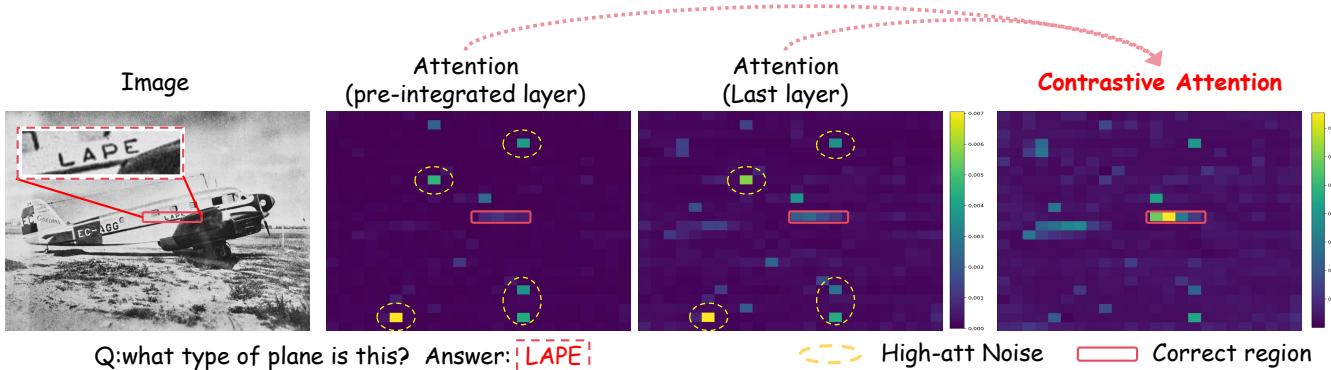


Figure 1: Contrastive attention (pre-integrated → last layer) showing focus shift and persistent high-attention noise.

Recent work such as DoLa (Chuang et al. 2024) has demonstrated that contrasting internal representations across layers can better reveal what the model truly learns. Specifically, DoLa computes the difference between the logits of early and later layers, producing *contrastive logits* that better reflect the model’s factual knowledge compared to relying solely on the final layer output. Inspired by this idea, we extend the notion of inter-layer contrast from output space to the attention space. In particular, we observe that as MLLMs process inputs layer by layer, their attention gradually shifts from task-irrelevant regions to more semantically meaningful areas. This shift reflects how the model integrates visual cues in a progressive manner. Shallow layers tend to contain noisy or indiscriminate attention, while deeper layers refine this focus toward task-relevant content. We refer to this evolving focus as **contrastive attention**, which captures not the static attention at any single layer, but the transformation in attention patterns across layers that *reveals what the model incrementally learns to attend to*.

To quantify the contrastive attention, we introduce two layer concepts: (a) *the post-integrated layer*, where the model has already combined visual and linguistic information and formed a representation capable of solving the task. We identify the post-integrated layer as the one immediately preceding the review layer (see section 5.4 for detailed exploration). (b) *the pre-integrated layer*, which represents the initial perception of the image before substantial semantic fusion occurs. The pre-integrated layer is selected from the identified fusion layers as the one whose attention map exhibits the largest Hellinger distance from the post-integrated layer, indicating the point before major vision-language integration takes place (see section 5.5).

Based on the above analysis, we introduce a training-free approach to enhance vision-language understanding of MLLMs. Specifically, we compute the contrastive attention by comparing attention maps between the pre-integrated layer and the post-integrated layer. It captures the actual contribution of visual information as it flows through the model, revealing how visual semantics are progressively integrated. Moreover, it effectively suppresses spurious high-attention noise in later layers. Then we apply contrastive attention at review layer to mask visual regions. This selec-

tive masking reduces the influence of irrelevant content and enables the model to concentrate more effectively on task-relevant areas without additional training. Experiments show that our method significantly improves the performance of the widely used LLaVA series across six visual question answering benchmarks, achieving state-of-the-art results. Our contributions are as follows:

- We conduct a systematic investigation into how visual information is integrated across layers in MLLMs. By applying layer-wise visual masking, we identify key visual-textual fusion layers and a review-like mechanism.
- We propose a training-free method that exploits contrastive attention, the divergence between pre-integrated and post-integrated attention maps, to refine visual focus.
- Our method consistently outperforms existing techniques and achieves state-of-the-art results across multiple multimodal benchmarks, validating its generality and effectiveness.

2 Related Work

Early efforts to understand how information flows within language models primarily focused on transformers in unimodal settings. For example, studies like (Cao et al. 2020; Frank, Bugliarello, and Elliott 2021) analyzed how attention mechanisms propagate syntactic and semantic information in transformers, while others (Aflalo et al. 2022; Chefer, Gur, and Wolf 2021; Lyu et al. 2022; Stan et al. 2024) explored the roles of feed-forward networks and memory representation in information transformation. These works provided foundational insights into token-level dependency and hierarchical abstraction but largely focused on language-only settings. Building on this, recent studies examined how LLMs acquire knowledge across layers. Lin et al. (2025) investigates the impact of visual fusion positions on MLLM performance, comparing external and internal integration strategies for incorporating visual information. Jin et al. (2024) introduced the concept of “depth” in reasoning, and Ju et al. (2024) showed context is unevenly distributed across layers.

A growing body of work has recently turned to the interpretability of MLLMs. For example, Palit et al. (2023)

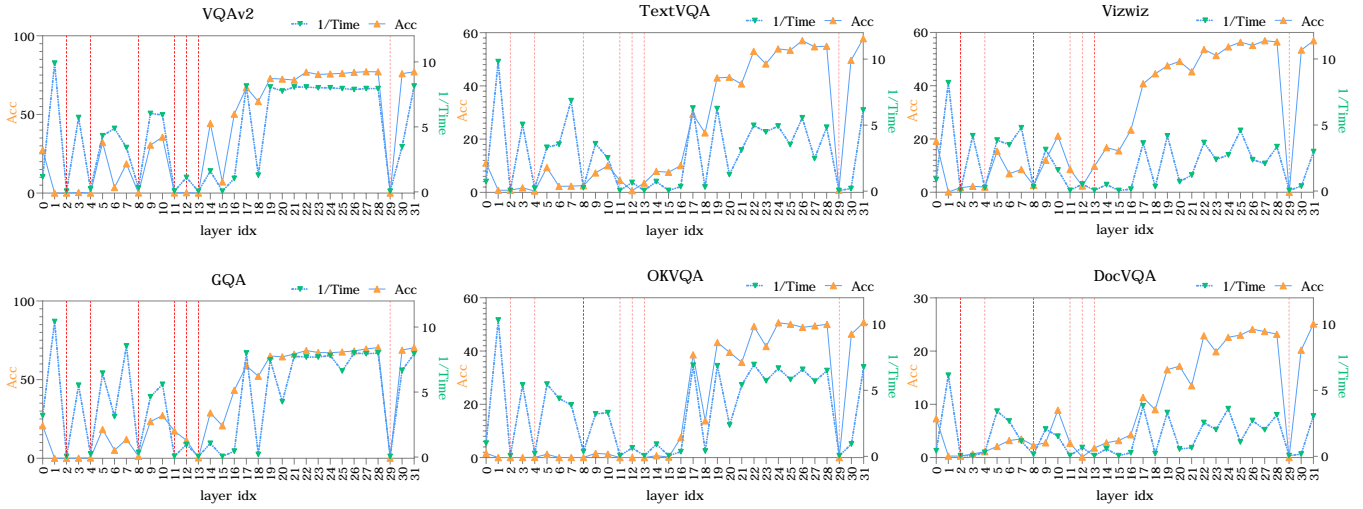


Figure 2: Layer-wise masking effects on accuracy and inference time across multimodal datasets using LLaVA-1.5. Acc is the performance after completely masking the visual information at the corresponding layer.

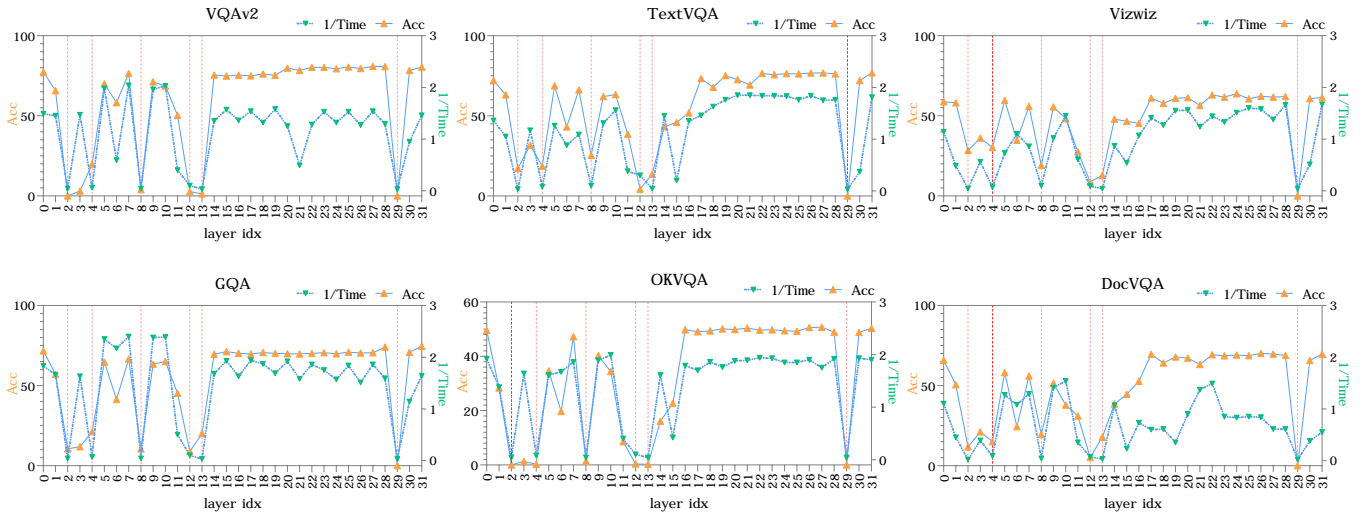


Figure 3: Layer-wise masking effects on accuracy and inference time across multimodal datasets using LLaVA-1.6.

extended causal tracing methods to MLLMs and showed that visual information progressively influences generation in later layers. Zhao et al. (2024) surveyed various interpretability techniques for MLLMs, categorizing insights at input, token, and attention levels. However, most of these efforts focus on saliency or input-output attribution and rarely dissect the internal fusion mechanism of visual features across layers. Despite these efforts, what remains largely missing is a comprehensive understanding of how visual information is gradually injected and transformed across different layers within MLLMs. Existing works often rely on single-layer attention analysis or fixed fusion strategies, overlooking the progressive, multi-stage nature of visual integration. A comprehensive understanding of how visual information is progressively injected across layers in MLLMs is still lacking. This gap limits both interpretability and usage of MLLMs in complex vision-language tasks.

3 Exploration of Visual Information Fusion

3.1 Layer-wise Visual Information Masking

To better understand how multimodal information flows and is integrated across layers in MLLMs, we conduct a series of layer-wise image masking experiments on the LLaVA series. Specifically, we follow the input format used in LLaVA and identify the position of image tokens based on the special marker `<image>`. In LLaVA, which uses a ViT-based image encoder, the number of image tokens is 576, allowing us to locate the image segment within the input sequence. Thus, we apply a masking operation to the image tokens at each layer by directly setting their embeddings to zero, effectively removing visual information while preserving the input shape. We then assess how each layer depends on image features by measuring performance changes across datasets. A significant drop in performance after masking indicates

that the layer relies heavily on image for multimodal integration. The results are shown in Figure 2 and 3.

3.2 Analysis and Observations

Layer-wise Differences in Visual-Language Fusion. Our results show that masking visual information at shallow layers (layers 0–4) leads to a sharp performance drop across all datasets. This suggests that image features are not yet integrated into the multimodal representations at early layers. Removing image at these layers deprives the model of essential visual cues, severely affecting its output. As the layer depth increases, the model begins to incorporate visual information gradually. The layer at which this integration completes varies by dataset: (1) For simple tasks like VQAv2, image-text fusion appears to complete earlier, as performance stabilizes after around layer 16. (2) For complex tasks such as OKVQA, the integration occurs at deeper layers, suggesting that more abstract reasoning requires longer propagation of visual context. In summary, masking the image after layer 19 results in no substantial performance degradation, indicating that the visual semantics have already been sufficiently integrated.

Identifying Critical Fusion Layers. In the layer-wise masking experiments, we find that masking visual information at certain specific layers leads to a dramatic drop in model performance, sometimes approaching zero. Notably, these critical layers show strong consistency across different datasets and across various MLLMs, indicating that the same set of layers consistently exhibits such behavior under different settings. Furthermore, we observe that masking at these layers not only degrades performance but also significantly increases inference time (measured as $1/t$). We hypothesize that this results from the disruption of efficient reasoning pathways within the model. These critical layers could be categorized into two groups:

- Early fusion layers ($S = 2, 4, 8, 11, 12, 13$): These critical layers are mostly located in the shallow stages of the model, where visual information has not yet been fully fused with textual input. Masking at these layers removes essential visual cues, leading to a sharp performance drop, indicating active fusion is still in progress.
- Review layer (29): After the early fusion layers, model performance stabilizes and becomes largely insensitive to visual masking, suggesting that fusion is mostly complete. However, at layer 29, masking again causes a significant drop, resembling the behavior of early fusion layers. We hypothesize that this layer performs a “final visual check” before the model generates its output. This mirrors human behavior, where one might glance back at the image one last time before making a decision.

The experiment reveals key phenomena: hierarchical differences in visual information fusion and the presence of critical fusion layer. Specifically, we observe: (1) A set of shallow layers serve as essential **early fusion layers** for integrating multimodal information. (2) At a deep layer (review layer), the LLM exhibits a **review-like** behavior, where visual information is revisited even after the integration pro-

cess has been completed. This suggests that the model still relies on visual cues for final decision verification.

4 Method

As shown in Figure 4, we compute the **contrastive attention** by selecting appropriate pre-integrated and post-integrated layers, in section 4.1. The contrastive attention is defined as the difference in attention distribution, capturing how attention shifts as visual information is fused. Then, in section 4.2, we leverage the contrastive attention to guide the **review** process, helping suppress irrelevant information and focus on content that is more relevant to the task.

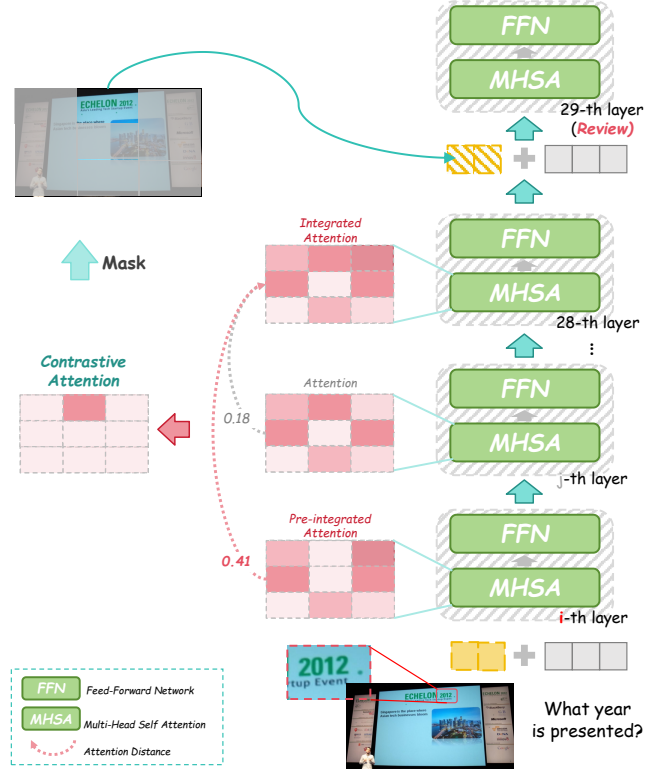


Figure 4: overview of contrastive attention and review-stage masking.

4.1 Selecting Contrastive Layers

To investigate how the attention shifts during the process of task understanding, we explore two contrastive layers: the post-integrated layer and the pre-integrated layer. The post-integrated layer represents the stage at which task semantics and visual information have been fully fused, while the pre-integrated layer captures the initial perception of the image. By comparing attention maps at these two layers, we aim to reveal which image regions become increasingly aligned with task objectives. We begin by locating the post-integrated layer. Experiment shows that review behavior occurs at layer 29. Layer 28 masking has minimal impact on performance, indicating that the fusion of visual features is

largely complete. Thus, we designate layer 28 as the post-integrated layer.

MLLMs form an initial, task-agnostic perception of the image at shallow layers, which may lead to high-attention noise unrelated to task. To mitigate this, we propose contrastive attention, which captures the difference between the attention maps of the post-integrated layer and a pre-integrated layer. This difference is designed to suppress irrelevant high-attention regions and enhance task-relevant visual focus. We compute the Hellinger distance between each layer’s attention map and that of the post-integrated layer, and select the one with the highest distance as the pre-integrated layer. We explore multiple strategies to define the candidate set \mathcal{C} for selecting the pre-integrated layer: (a) without any constraint, (b) constrained to shallow layers (layers 1–16), (c) constrained to deep layers (layers 17–28), and (d) constrained to a predefined early fusion set \mathcal{S} identified through our analysis. Details are provided in Table 3 and section 5.5.

We formalize the selection process as follows: given a set of candidate attention matrices $A^{(i)}$, where each $A^{(i)} \in \mathbb{R}^{d \times d}$ represents the attention weights at layer i , we define the attention at the post-integrated layer (layer $k = 28$) as $A^{(k)}$. To identify the attention matrix that deviates most significantly from $A^{(k)}$ in terms of distributional difference, we compute the Hellinger distance between each $A^{(i)}$ and the reference $A^{(k)}$, and select the one with the maximal distance from candidate layers \mathcal{C} :

$$i^* = \arg \max_{i \in \mathcal{C}} H(A^{(i)}, A^{(k)}) \quad (1)$$

where $H(P, Q)$ denotes the Hellinger distance between two probability distributions P and Q , defined as:

$$H(P, Q) = \frac{1}{\sqrt{2}} \sqrt{\sum_{j=1}^d (\sqrt{p_j} - \sqrt{q_j})^2} \quad (2)$$

where d denotes the number of image tokens involved in the attention distribution.

4.2 Contrastive Attention for Review

As shown in Figure 4, we leverage the observed layer-wise fusion phenomenon in MLLMs, particularly the review-like behavior, where the model reattends to the image even after the primary fusion appears to be completed. Based on this, we apply the contrastive attention to guide the masking of visual information during this review stage. Specifically, the *contrastive attention* is computed as the difference between the attention at pre-integrated layer $\mathbf{A}^{(i^*)}$ and that at post-integrated layer $\mathbf{A}^{(k)}$.

$$\text{IA} = |\mathbf{A}^{(k)} - \mathbf{A}^{(i^*)}| \quad (3)$$

The difference between the attention from the pre-integrated layer and the post-integrated layer captures how visual information shifts the attention during the visual integration and understanding. We leverage this signal to refine the model’s attention at review layer through a soft masking

strategy. Specifically, we identify visual tokens whose contrastive attention scores fall below the ρ -th percentile and softly suppress their influence by scaling down features. Formally, let $Q_\rho(\text{IA})$ denote the ρ -th quantile of the contrastive attention scores IA . The masked visual features are computed as:

$$\mathbf{E}_j^{\text{masked}} = \lambda \cdot \mathbf{E}_j, \quad \text{if } \text{IA}_j < Q_\rho(\text{IA}) \quad (4)$$

where \mathbf{E}_j is the embedding of the j -th visual token, and $\lambda \ll 1$ is a constant that softly downweights low-relevance regions without fully discarding them. We analyze the effect of varying the masking ratio ρ in section 5.6.

5 Experiments

5.1 Datasets and Setting

The proposed method is evaluated on six widely-used multimodal datasets: VQAv2 (Goyal et al. 2017), GQA (Hudson and Manning 2019), TextVQA (Singh et al. 2019), OKVQA (Marino et al. 2019), VizWiz (Gurari et al. 2018), and DocVQA (Mathew, Karatzas, and Jawahar 2021). We report accuracy on each dataset as the evaluation metric. All experiments are conducted based on the open-source and SOTA LLaVA series (Liu et al. 2023, 2024): LLaVA-1.5-7B, LLaVA-1.6-Vicuna-7B. The experiments were conducted on an RTX A800 GPU using PyTorch 2.0, and the system was based on Ubuntu 20.04.

5.2 Comparison with MLLMs

The baseline MLLMs include BLIP-2 (Li et al. 2023), Flamingo (Alayrac et al. 2022), InstructBLIP (Dai et al. 2023), IDEFICS (Laurenç̄on et al. 2023), LLaVA (Liu et al. 2023), LLaVA-1.5 (Liu et al. 2024), InternVL-MLP (Chen et al. 2024), InternVL-QLLaMA (Chen et al. 2024), and Qwen-VL (Bai et al. 2023). As shown in Table 1, integrating our method into LLaVA-1.5 yields state-of-the-art performance across six VQA benchmarks, achieving an average score of 58.17. This surpasses strong recent baselines such as InternVL-MLP (52.97) and Qwen-VL (50.49).

5.3 Comparison with Training-free Methods

To evaluate the effectiveness of our proposed training-free method, as shown in Table 2, we also compare it against two representative methods: (1) *DoLA* (Chuang et al. 2024) proposes a training-free decoding strategy that contrasts the output logits between earlier and later transformer layers, amplifying deep-layer factual knowledge and reducing hallucination without requiring additional supervision. (2) *ViCrop* (Zhang et al. 2025) introduces a training-free adversarial framework that manipulates image inputs by strategically masking and cropping regions to challenge the visual reasoning of MLLMs, revealing their sensitivity to localized visual changes.

As illustrated in Table 2, our approach consistently outperforms existing representative methods, demonstrating improved stability and transferability during inference. These results indicate that contrastive attention effectively identifies and enhances critical visual regions, providing a

Table 1: Effectiveness of our method across multiple MLLM baselines.

MLLMs	GQA	VQAv2	OKVQA	VizWiz	TextVQA	DocVQA	Average
BLIP-2 (Li et al. 2023)	41.0	41.0	45.9	19.6	42.5	-	38.00
Flamingo-80B (Alayrac et al. 2022)	43.3	56.3	50.6	31.6	-	-	45.45
InstructBILP-8B (Dai et al. 2023)	49.2	51.9	49.9	34.5	50.1	9.2	40.80
IDEFICS (Laurençon et al. 2023)	38.4	50.9	38.4	35.5	25.9	-	37.82
LLaVA (Liu et al. 2023)	49.5	63.6	45.2	30.7	38.9	10.5	39.72
InternVL-MLP (Chen et al. 2024)	62.9	79.3	42.9	52.5	57.0	23.2	52.97
InternVL-QLLaMA (Chen et al. 2024)	57.7	72.3	51.0	44.5	42.1	25.0	48.77
Qwen-VL (Bai et al. 2023)	59.3	78.8	46.9	35.2	57.2	25.5	50.49
Qwen2-VL (Wang et al. 2024)	63.7	79.8	48.5	60.4	71.9	59.8	64.02
<i>LLaVA-v1.5</i> (Liu et al. 2023)	66.0	74.0	51.6	57.8	57.2	24.6	55.19
+ <i>Ours</i>	69.4	77.6	55.4	60.4	59.8	26.9	58.25
<i>LLaVA-v1.6</i> (Liu et al. 2024)	69.3	79.9	52.5	59.6	72.0	65.8	66.52
+ <i>Ours</i>	71.6	80.7	56.9	62.0	75.8	68.1	69.18

Table 2: Effectiveness of contrastive attention compared to existing enhanced methods.

MLLMs	Methods	GQA	VQAv2	OKVQA	VizWiz	TextVQA	DocVQA	Average
<i>LLaVA-v1.5</i>	+ DoLA (Chuang et al. 2024)	66.8	70.1	52.8	58.4	56.1	26.0	55.04
	+ ViCrop (Zhang et al. 2025)	67.0	76.0	54.8	59.6	56.6	25.1	56.52
	+ <i>Ours</i>	69.4	77.6	55.4	60.4	59.8	26.9	58.25
<i>LLaVA-v1.6</i>	+ DoLA (Chuang et al. 2024)	71.0	75.4	53.6	60.9	72.1	67.2	66.69
	+ ViCrop (Zhang et al. 2025)	70.2	81.4	54.1	61.3	73.4	65.6	67.00
	+ <i>Ours</i>	71.6	80.7	56.9	62.0	75.8	68.1	69.18

lightweight yet effective enhancement to the inference process without requiring any additional training.

5.4 Selection of post-integrated layer

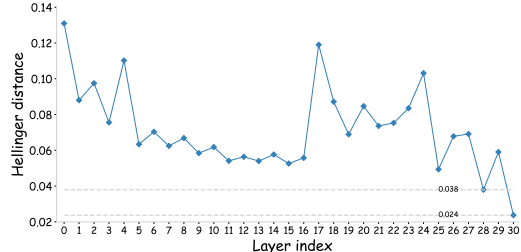


Figure 5: Layer-wise Hellinger distance to the final layer.

Before identifying the post-integrated layer for applying contrastive attention, we first clarify two key questions:

1. Where and how does contrastive attention function?
Contrastive attention functions by suppressing image regions that are irrelevant to the task. Our exploratory experiments show that image has little effect on deeper layers (e.g., beyond the 20th layer), where visual information has already been fully integrated. However, we observe that a secondary integration of visual and textual information occurs at layer 29, referred to as the “review” layer. Therefore, to influence

the final reasoning, **contrastive attention should take effect at layer 29**.

2. Why is layer 28 selected as the post-integrated layer?

While the final layer (layer 31) represents the model’s fully aggregated understanding, it cannot be directly used for contrastive attention. This is because contrastive attention must be computed before layer 29 in order to take effect at the point where visual-textual fusion reoccurs. Therefore, **the post-integrated layer needs to be selected before layer 29**. To approximate the role of the final layer, we calculate the Hellinger Distance between the attention distributions of each layer and that of layer 31. The results show that both layer 28 and layer 30 exhibit minimal distance from the final layer, indicating that their attention patterns closely resemble the final attention. Thus, we select layer 28 as the post-integrated layer for computing contrastive attention.

5.5 Selection of Pre-Integrated Layers

We systematically explored different strategies for selecting the pre-integrated layer, considering four selection scope from: (a) *all* layers (unconstrained setting, 0–28), (b) *deep* layers (16–28), (c) *shallow* layers (0–16), and (d) the set of *fusion* layers (2, 4, 8, 11, 12, 13) identified in section 3.2.

The pre-integrated layer refers to the stage where visual information is initially processed, before being influenced by textual context. Therefore, layers with already fused representations should be excluded. As shown in Table 3, the

Table 3: Pre-integrated layer selection on LLaVA-v1.5-7B.

	GQA	VQAv2	OKVQA	VizWiz	TextVQA	DocVQA	Average
all (0-28)	65.40	72.97	51.34	57.77	52.50	26.10	54.35
deep (16-28)	60.30	70.11	52.80	57.40	56.10	26.00	53.79
shallow (0-15)	68.30	76.49	53.92	59.30	57.00	26.40	56.90
fusion (\mathcal{S})	69.40	77.59	55.40	60.40	59.80	26.90	58.25

deep strategy performs poorly because these layers contain cross-modal information, which degrades the quality of contrastive attention. Similarly, the *all* strategy includes deep layers, introducing noisy and biased attention. In comparison, the *shallow* strategy achieves better results. The best performance comes from the *fusion* strategy, which limits selection to empirically identified fusion layers \mathcal{S} .

As shown in Figure 6, we further investigate the distribution of automatically selected pre-integrated layers when no constraints are imposed on the selection range. Specifically, we apply Equation (1) to identify the layer that exhibits the largest attention divergence from the post-integrated layer. As illustrated, layer 2 is selected with overwhelmingly high frequency across all datasets, indicating a strong concentration around this early layer. For instance, in DocVQA, over 86% of samples select layer 2 as the pre-integrated layer. Figure 6 shows that fusion layers \mathcal{S} are favored as pre-integrated layers, reinforcing our claim that they are well-suited for contrastive attention.

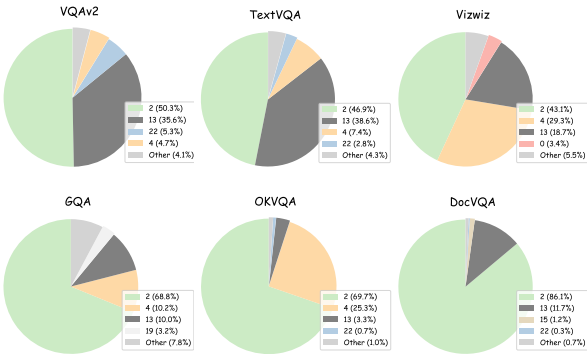


Figure 6: Distribution of selected pre-integrated layers across tasks under unconstrained candidate setting.

5.6 Masking Ratio Based on Contrastive Attention

Based on the observed review-like behavior, we applied contrastive attention at review layer of the MLLM and used a soft mask strategy to selectively suppress irrelevant visual information. In this section, we investigate how different masking ratios affect model performance and efficiency. As shown in Figure 7, we evaluated the accuracy and inference time across six benchmarks under varying mask ratios on LLaVA-1.5. We observe a consistent trend: accuracy peaks when 20% of the tokens are masked, but degrades as the masking ratio increases further. Meanwhile, inference time

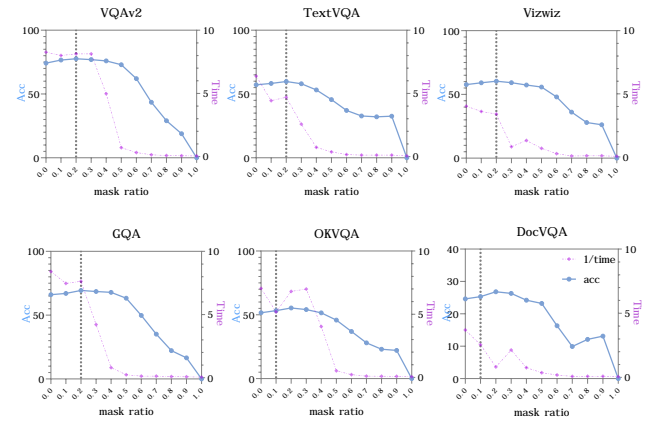


Figure 7: Effect of visual token masking ratio on accuracy and inference time at the review layer.

decreases steadily as the masking ratio increases. When the masking ratio reaches 1.0—i.e., the model receives no visual input—the accuracy drops to zero on all datasets. This clearly confirms the critical role of visual signals at the review layer during final-stage reasoning.

6 Conclusion

In this paper, we present a systematic analysis of visual information integration in MLLMs by conducting layer-wise masking experiments. Our findings reveal that visual-text fusion primarily occurs in a certain number of shallow layers, while a review-like re-attention behavior emerges just before the final output. Building on these findings, we propose a training-free method that enhances vision-language reasoning using contrastive attention. This attention is computed by comparing the attention maps between a pre-integrated layer, which represents early visual perception, and a post-integrated layer, where vision and language are fully fused. The resulting contrastive signal reveals the model’s evolving visual focus and helps suppress irrelevant high-attention noise in later layers. When applied at the review layer, this approach guides the model to concentrate on task-relevant visual regions more effectively, without any additional training. Extensive experiments across six VQA benchmarks demonstrate that our method consistently improves the performance of LLaVA series models, achieving new state-of-the-art results. Our work provides deeper insight into the internal mechanisms of MLLMs and offers a lightweight, effective strategy for enhancing multimodal understanding.

References

Aflalo, E.; Du, M.; Tseng, S.-Y.; Liu, Y.; Wu, C.; Duan, N.; and Lal, V. 2022. Vi-interpret: An interactive visualization tool for interpreting vision-language transformers. In *Proceedings of the IEEE/CVF Conference on computer vision and pattern recognition*, 21406–21415.

Alayrac, J.-B.; Donahue, J.; Luc, P.; Miech, A.; Barr, I.; Hasson, Y.; Lenc, K.; Mensch, A.; Millican, K.; Reynolds, M.; et al. 2022. Flamingo: a visual language model for few-shot learning. *Advances in neural information processing systems*, 35: 23716–23736.

Bai, J.; Bai, S.; Yang, S.; Wang, S.; Tan, S.; Wang, P.; Lin, J.; Zhou, C.; and Zhou, J. 2023. Qwen-VL: A Versatile Vision-Language Model for Understanding, Localization, Text Reading, and Beyond. *arXiv preprint arXiv:2308.12966*.

Cao, J.; Gan, Z.; Cheng, Y.; Yu, L.; Chen, Y.-C.; and Liu, J. 2020. Behind the scene: Revealing the secrets of pre-trained vision-and-language models. In *Computer Vision–ECCV 2020: 16th European Conference, Glasgow, UK, August 23–28, 2020, Proceedings, Part VI 16*, 565–580. Springer.

Chefer, H.; Gur, S.; and Wolf, L. 2021. Generic attention-model explainability for interpreting bi-modal and encoder-decoder transformers. In *Proceedings of the IEEE/CVF international conference on computer vision*, 397–406.

Chen, Z.; Wu, J.; Wang, W.; Su, W.; Chen, G.; Xing, S.; Zhong, M.; Zhang, Q.; Zhu, X.; Lu, L.; et al. 2024. Internvl: Scaling up vision foundation models and aligning for generic visual-linguistic tasks. In *Proceedings of the IEEE/CVF conference on computer vision and pattern recognition*, 24185–24198.

Chuang, Y.-S.; Xie, Y.; Luo, H.; Kim, Y.; Glass, J.; and He, P. 2024. Dola: Decoding by contrasting layers improves factuality in large language models. *arXiv preprint arXiv:2309.03883*.

Dai, W.; Li, J.; Li, D.; Tiong, A. M. H.; Zhao, J.; Wang, W.; Li, B.; Fung, P.; and Hoi, S. 2023. InstructBLIP: Towards General-purpose Vision-Language Models with Instruction Tuning. *arXiv:2305.06500*.

Frank, S.; Bugliarello, E.; and Elliott, D. 2021. Vision-and-language or vision-for-language? on cross-modal influence in multimodal transformers. *arXiv preprint arXiv:2109.04448*.

Goyal, Y.; Khot, T.; Summers-Stay, D.; Batra, D.; and Parikh, D. 2017. Making the v in vqa matter: Elevating the role of image understanding in visual question answering. In *Proceedings of the IEEE conference on computer vision and pattern recognition*, 6904–6913.

Gurari, D.; Li, Q.; Stangl, A. J.; Guo, A.; Lin, C.; Grauman, K.; Luo, J.; and Bigham, J. P. 2018. Vizwiz grand challenge: Answering visual questions from blind people. In *Proceedings of the IEEE conference on computer vision and pattern recognition*, 3608–3617.

Hudson, D. A.; and Manning, C. D. 2019. Gqa: A new dataset for real-world visual reasoning and compositional question answering. In *Proceedings of the IEEE/CVF conference on computer vision and pattern recognition*, 6700–6709.

Jin, M.; Yu, Q.; Huang, J.; Zeng, Q.; Wang, Z.; Hua, W.; Zhao, H.; Mei, K.; Meng, Y.; Ding, K.; et al. 2024. Exploring Concept Depth: How Large Language Models Acquire Knowledge and Concept at Different Layers? *arXiv preprint arXiv:2404.07066*.

Ju, T.; Sun, W.; Du, W.; Yuan, X.; Ren, Z.; and Liu, G. 2024. How large language models encode context knowledge? a layer-wise probing study. *arXiv preprint arXiv:2402.16061*.

Laurençon, H.; Saulnier, L.; Tronchon, L.; Bekman, S.; Singh, A.; Lozhkov, A.; Wang, T.; Karamcheti, S.; Rush, A.; Kiela, D.; et al. 2023. Obelics: An open web-scale filtered dataset of interleaved image-text documents. *Advances in Neural Information Processing Systems*, 36: 71683–71702.

Li, J.; Li, D.; Savarese, S.; and Hoi, S. 2023. Blip-2: Bootstrapping language-image pre-training with frozen image encoders and large language models. In *International conference on machine learning*, 19730–19742. PMLR.

Lin, J.; Chen, H.; Fan, Y.; Fan, Y.; Jin, X.; Su, H.; Fu, J.; and Shen, X. 2025. Multi-Layer Visual Feature Fusion in Multimodal LLMs: Methods, Analysis, and Best Practices. *arXiv preprint arXiv:2503.06063*.

Liu, H.; Li, C.; Li, Y.; and Lee, Y. J. 2024. Improved Baselines with Visual Instruction Tuning.

Liu, H.; Li, C.; Wu, Q.; and Lee, Y. J. 2023. Visual Instruction Tuning.

Lyu, Y.; Liang, P. P.; Deng, Z.; Salakhutdinov, R.; and Morency, L.-P. 2022. Dime: Fine-grained interpretations of multimodal models via disentangled local explanations. In *Proceedings of the 2022 AAAI/ACM Conference on AI, Ethics, and Society*, 455–467.

Marino, K.; Rastegari, M.; Farhadi, A.; and Mottaghi, R. 2019. Ok-vqa: A visual question answering benchmark requiring external knowledge. In *Proceedings of the IEEE/cvf conference on computer vision and pattern recognition*, 3195–3204.

Mathew, M.; Karatzas, D.; and Jawahar, C. 2021. Docvqa: A dataset for vqa on document images. In *Proceedings of the IEEE/CVF winter conference on applications of computer vision*, 2200–2209.

Palit, V.; Pandey, R.; Arora, A.; and Liang, P. P. 2023. Towards vision-language mechanistic interpretability: A causal tracing tool for blip. In *Proceedings of the IEEE/CVF International Conference on Computer Vision*, 2856–2861.

Singh, A.; Natarajan, V.; Shah, M.; Jiang, Y.; Chen, X.; Batra, D.; Parikh, D.; and Rohrbach, M. 2019. Towards vqa models that can read. In *Proceedings of the IEEE/CVF conference on computer vision and pattern recognition*, 8317–8326.

Stan, G. B. M.; Aflalo, E.; Rohekar, R. Y.; Bhiwandiwalla, A.; Tseng, S.-Y.; Olson, M. L.; Gurwicz, Y.; Wu, C.; Duan, N.; and Lal, V. 2024. LVLM-Interpret: An Interpretability Tool for Large Vision-Language Models. *arXiv preprint arXiv:2404.03118*.

Wang, P.; Bai, S.; Tan, S.; Wang, S.; Fan, Z.; Bai, J.; Chen, K.; Liu, X.; Wang, J.; Ge, W.; et al. 2024. Qwen2-vl: Enhancing vision-language model’s perception of the world at any resolution. *arXiv preprint arXiv:2409.12191*.

Zhang, J.; Khayatkhoei, M.; Chhikara, P.; and Ilievski, F. 2025. MLLMs know where to look: Training-free perception of small visual details with multimodal LLMs. *arXiv preprint arXiv:2502.17422*.

Zhao, Q.; Xu, M.; Gupta, K.; Asthana, A.; Zheng, L.; and Gould, S. 2024. The first to know: How token distributions reveal hidden knowledge in large vision-language models? In *European Conference on Computer Vision*, 127–142. Springer.

Reproducibility Checklist

Instructions for Authors:

This document outlines key aspects for assessing reproducibility. Please provide your input by editing this `.tex` file directly.

For each question (that applies), replace the “Type your response here” text with your answer.

Example: If a question appears as

```
\question{Proofs of all novel claims  
are included} { (yes/partial/no) }  
Type your response here
```

you would change it to:

```
\question{Proofs of all novel claims  
are included} { (yes/partial/no) }  
yes
```

Please make sure to:

- Replace ONLY the “Type your response here” text and nothing else.
- Use one of the options listed for that question (e.g., **yes**, **no**, **partial**, or **NA**).
- **Not** modify any other part of the `\question` command or any other lines in this document.

You can `\input` this `.tex` file right before `\end{document}` of your main file or compile it as a stand-alone document. Check the instructions on your conference’s website to see if you will be asked to provide this checklist with your paper or separately.

1. General Paper Structure

- 1.1. Includes a conceptual outline and/or pseudocode description of AI methods introduced (yes/partial/no/NA) **yes**
- 1.2. Clearly delineates statements that are opinions, hypothesis, and speculation from objective facts and results (yes/no) **yes**
- 1.3. Provides well-marked pedagogical references for less-familiar readers to gain background necessary to replicate the paper (yes/no) **yes**

2. Theoretical Contributions

- 2.1. Does this paper make theoretical contributions? (yes/no) **yes**

If yes, please address the following points:

- 2.2. All assumptions and restrictions are stated clearly and formally (yes/partial/no) **yes**
- 2.3. All novel claims are stated formally (e.g., in theorem statements) (yes/partial/no) **yes**

- 2.4. Proofs of all novel claims are included (yes/partial/no) **yes**
- 2.5. Proof sketches or intuitions are given for complex and/or novel results (yes/partial/no) **yes**
- 2.6. Appropriate citations to theoretical tools used are given (yes/partial/no) **yes**
- 2.7. All theoretical claims are demonstrated empirically to hold (yes/partial/no/NA) **yes**
- 2.8. All experimental code used to eliminate or disprove claims is included (yes/no/NA) **yes**

3. Dataset Usage

- 3.1. Does this paper rely on one or more datasets? (yes/no) **yes**

If yes, please address the following points:

- 3.2. A motivation is given for why the experiments are conducted on the selected datasets (yes/partial/no/NA) **yes**
- 3.3. All novel datasets introduced in this paper are included in a data appendix (yes/partial/no/NA) **NA**
- 3.4. All novel datasets introduced in this paper will be made publicly available upon publication of the paper with a license that allows free usage for research purposes (yes/partial/no/NA) **NA**
- 3.5. All datasets drawn from the existing literature (potentially including authors’ own previously published work) are accompanied by appropriate citations (yes/no/NA) **yes**
- 3.6. All datasets drawn from the existing literature (potentially including authors’ own previously published work) are publicly available (yes/partial/no/NA) **yes**
- 3.7. All datasets that are not publicly available are described in detail, with explanation why publicly available alternatives are not scientifically satisfying (yes/partial/no/NA) **NA**

4. Computational Experiments

- 4.1. Does this paper include computational experiments? (yes/no) **yes**

If yes, please address the following points:

- 4.2. This paper states the number and range of values tried per (hyper-) parameter during development of the paper, along with the criterion used for selecting the final parameter setting (yes/partial/no/NA) **yes**
- 4.3. Any code required for pre-processing data is included in the appendix (yes/partial/no) **yes**

- 4.4. All source code required for conducting and analyzing the experiments is included in a code appendix (yes/partial/no) **yes**
- 4.5. All source code required for conducting and analyzing the experiments will be made publicly available upon publication of the paper with a license that allows free usage for research purposes (yes/partial/no) **yes**
- 4.6. All source code implementing new methods have comments detailing the implementation, with references to the paper where each step comes from (yes/partial/no) **yes**
- 4.7. If an algorithm depends on randomness, then the method used for setting seeds is described in a way sufficient to allow replication of results (yes/partial/no/NA) **yes**
- 4.8. This paper specifies the computing infrastructure used for running experiments (hardware and software), including GPU/CPU models; amount of memory; operating system; names and versions of relevant software libraries and frameworks (yes/partial/no) **yes**
- 4.9. This paper formally describes evaluation metrics used and explains the motivation for choosing these metrics (yes/partial/no) **yes**
- 4.10. This paper states the number of algorithm runs used to compute each reported result (yes/no) **yes**
- 4.11. Analysis of experiments goes beyond single-dimensional summaries of performance (e.g., average; median) to include measures of variation, confidence, or other distributional information (yes/no) **no**
- 4.12. The significance of any improvement or decrease in performance is judged using appropriate statistical tests (e.g., Wilcoxon signed-rank) (yes/partial/no) **no**
- 4.13. This paper lists all final (hyper-)parameters used for each model/algorithm in the paper's experiments (yes/partial/no/NA) **yes**